Origin of Fine Structure in Si 2p Photoelectron Spectra at Silicon Surfaces and Interfaces

Oleg V. Yazyev[1] and Alfredo Pasquarello[2,3]

[1]*Ecole Polytechnique Fédérale de Lausanne (EPFL), Institute of Chemical Sciences and Engineering, CH-1015 Lausanne, Switzerland*
[2]*Ecole Polytechnique Fédérale de Lausanne (EPFL), Institute of Theoretical Physics, CH-1015 Lausanne, Switzerland*
[3]*Institut Romand de Recherche Numérique en Physique des Matériaux (IRRMA), CH-1015 Lausanne, Switzerland*
(Received 12 September 2005; published 19 April 2006)

Using a first-principles approach, we investigate the origin of the fine structure in Si 2p photoelectron spectra at the Si(100)-(2 × 1) surface and at the Si(100)-SiO_2 interface. Calculated and measured shifts show very good agreement for both systems. By using maximally localized Wannier functions, we clearly identify the shifts resulting from the electronegativity of second-neighbor atoms. The other shifts are then found to be proportional to the average bond-length variation around the Si atom. Hence, in combination with accurate modeling, photoelectron spectroscopy can provide a direct measure of the strain field at the atomic scale.

DOI: 10.1103/PhysRevLett.96.157601 PACS numbers: 79.60.−i, 68.35.−p, 73.20.−r

The increasing availability of synchrotron radiation facilities is bearing x-ray photoemission spectra of unprecedented resolution characterizing surfaces and interfaces [1]. The achieved sensitivity is sufficient to distinguish inequivalent subsurface atoms with identically composed first-neighbor shells. Hence, the interpretation of such core-level spectra can no longer be achieved with simple electronegativity arguments, but requires the consideration of the interplay between local strain fields and electronegativity effects of second-nearest neighbors. Thus, the challenges for theory not only involve the accuracy of computer simulations, but also the search for new paradigms to analyze the origin of the observed shifts.

These difficulties are strikingly illustrated for the Si(100)-(2 × 1) surface, which has been the object of numerous highly resolved x-ray photoemission investigations [2–5]. While the shifts pertaining to the first-layer dimer atoms have been identified [2,6], the other lines appearing in highly resolved Si 2p spectra still lack a consensual assignment [5], despite the detailed knowledge of the surface reconstruction [7–9]. Even more interesting is the case of the Si(100)-SiO_2 interface, where the atomic structure connecting the crystalline Si with the amorphous oxide remains a debated issue [10–12]. While the partial oxidation states of Si [13] are by now well understood [14], highly resolved spectra show fine structure in the nonoxidized Si line, with extra components at lower (Si^{α}) and higher binding energy (Si^{β}) with respect to the Si bulk line [15–17]. These lines result from substrate Si atoms in the neighborhood of the interface, but the cause of their appearance has remained obscure. Understanding their origin might shed light on the bonding pattern at this technologically relevant interface [12,17].

We here investigate the origin of the fine structure in Si 2p photoemission spectra at silicon surfaces and interfaces. At the Si(100)-(2 × 1) surface, our calculated shifts account for the experimental data and show that at least three Si layers are detected. Our interpretation highlights a linear relation between shifts and bond lengths. Adopting a recently generated model structure [10], we calculate Si 2p shifts at the Si(100)-SiO_2 interface and find quantitative agreement with experimental data, for both oxidized (Si^{+n}, with $n = 1, \ldots, 4$) and nonoxidized Si atoms (Si^{α}, Si^{β}). Having recourse to maximally localized Wannier functions [18], we clarify the origin of the fine structure, identifying the respective roles of second-neighbor O atoms and of local strain. The shift associated to the Si^{β} line is found to give a direct measure of substrate distortions at the Si(100)-SiO_2 interface.

Electronic-structure calculations and structural relaxations were performed within the local density approximation (LDA) to density functional theory. Only valence electrons were explicitly described and core-valence interactions were accounted for through pseudopotentials (PPs) [19]. We used a normconserving PP for Si [20] and an ultrasoft one for O [21]. The electron wave functions were described by plane-wave basis sets determined by an energy cutoff of 25 Ry. The cutoff was increased to 35 Ry for systems with O atoms. The Brillouin zone could be sampled at the only Γ point, since all the investigated systems are of sufficiently large size.

To interpret the Si 2p photoelectron spectra at silicon surfaces and interfaces, it is necessary to evaluate core-level *shifts* with respect to the Si bulk line. Since these shifts mainly result from the relaxation of *valence* electron states, their accurate determination is possible within a PP scheme, which does not treat core electrons explicitly [6,14,22]. We calculated Si 2p shifts including the effect of core-hole relaxation by taking total energy differences between two separate self-consistent calculations. First, the ground-state energy is determined; then the PP of a given Si atom is replaced by another PP which simulates the presence of a screened 2p hole in its core [6]. Upon electron excitation, the atomic positions are not allowed to relax in accordance with the sudden approximation [6], and a neutralizing background is used to ensure overall charge

 © 2006 The American Physical Society

TABLE I. Silicon $2p$ core-level shifts associated to the central Si atom in $SiO_n(SiH_3)_4$, as calculated with PP and AE schemes. The shifts (in eV) are given with respect to the central Si atom in $Si(SiH_3)_4$.

n	1	2	3	4
PP	0.83	1.50	2.10	2.85
AE	0.82	1.48	2.08	2.82

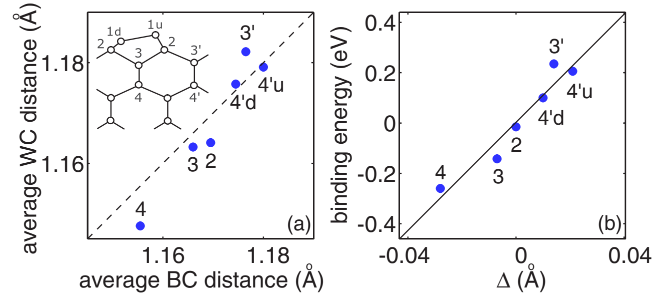

FIG. 1 (color online). Correlations for subsurface Si atoms at the Si(001)-$c(4 \times 2)$ surface: (a) average distance to the Wannier center (WC) vs average distance to the Si-Si bond center (BC); (b) Si $2p$ shift vs average Si-Si bond length given as deviation (Δ) with respect to the bulk (2.34 Å). The inset gives the adopted labeling. The $4'$ atoms can be further separated into inequivalent up ($4'u$) and down ($4'd$) atoms [30].

neutrality. Test calculations showed that *relative* Si $2p$ binding energies are negligibly affected when considering spin-polarized core holes or using generalized gradient approximations for the exchange-correlation energy [22]. Hence, all the shifts in this work were consistently determined in the LDA.

To illustrate the accuracy of our scheme, we focused on model molecules containing Si in various oxidation states [14], for which all-electron (AE) calculations could be performed [23]. In our AE calculations, the electronic state in the presence of a core hole was obtained by enforcing the occupation of the corresponding core orbital. We found deviations of at most 0.03 eV between PP and AE core-level shifts, over an energy range extending up to 3 eV (Table I). This comparison indicates that the PP scheme can give impressively accurate shifts for a series of similarly bonded atoms [22,25].

To understand the behavior of core-level shifts in the absence of important electronegativity effects, we first modeled the Si(100)-$c(4 \times 2)$ surface. We used a slab geometry in a periodically repeated simulation cell, consisting of 14 Si layers with a 4×4 repeat unit in the surface plane. The distance (8 Å) between the slab and its periodic images was taken sufficiently large to neglect spurious interactions. The eight lowest layers were kept fixed in bulk positions and their extremities were saturated with H atoms. Through structural relaxation, we recovered the well-known surface reconstruction consisting of alternating buckled dimers. The tilt angle in our calculation (19°) agrees well with both experimental measurements [9] and previous theoretical work [8]. The notation that we adopted to distinguish the Si atoms is given in Fig. 1.

In Table II, we give calculated binding energies for this surface structure, together with experimental data from various sources [2,3,5]. The calculated shifts for the dimer atoms agree well with experimental values and confirm previous assignments [6]. The second-layer atoms are found to yield very small shifts (-0.01 eV), noticeably smaller than in a previous calculation (0.13 eV) [6]. Third- and fourth-layer atoms give shifts to both lower (3, 4) and higher binding energies ($3'$, $4'$) with respect to the Si bulk line. Shifts of deeper layers are negligible.

These results lead us to propose a different interpretation than adopted so far in the literature (Table II). Second-layer atoms with their small shift are indistinguishable from the bulk. The clear experimental signatures at about 0.2 and -0.2 eV [2,3,5] then correspond to the two inequivalent atoms in the third layer, possibly with a contribution of fourth-layer atoms that behave similarly. The absence of shifts higher than 0.3 eV in our clean surface model is consistent with the experimental assignment of the high-binding-energy features to defects or surface loss structures [4,5].

In order to elucidate the origin of core-level shifts of subsurface atoms, we carried out an analysis in terms of maximally localized Wannier functions (MLWFs) [18], which conveniently represent the local electronic structure in a compact form. We focus on the initial state because core-hole relaxation effects are expected to scale linearly with the full shift for atoms in similarly bonded environments [14]. For a nonpolar Si-Si bond, the center of the corresponding MLWF coincides with the center of the bond. Therefore, a deviation between the positions of these two centers is an indicator of polarity in the bond. For each subsurface Si atom, we correlate in Fig. 1(a) the distances to these to centers and find overall good correspondence.

TABLE II. Calculated and measured Si $2p$ shifts at the Si(001)-$c(4 \times 2)$ surface. The shifts (in eV) are given with respect the Si bulk line. The theoretical reference is obtained from an average of deep Si atoms (5th–10th layer).

	Theory		Experiment	
	Present	Ref. [2]	Ref. [3]	Ref. [5]
$1u$	-0.49	-0.49	-0.49	-0.50
$1d$	0.02	0.06	0.06	0.06
2	-0.01			
3	-0.14	-0.21	-0.20	-0.21
4	-0.26			
$3'$	0.24	0.22	0.20	0.23
$4'u$	0.21			
$4'd$	0.10			

Hence, the polarity induced by ionic surface dimers is minor in subsurface layers.

The behavior of core-level shifts of subsurface atoms is understood through a simple correlation with Si-Si bond distances. For a given Si atom, the elongation of its bond distances leads to a decrease of the local electron density, resulting in a higher binding energy [26]. The validity of this correlation is demonstrated in Fig. 1(b), which gives the calculated shifts vs the average Si-Si distance to the four neighbor atoms. Therefore, the measured shift provides a direct indication of the local strain induced by the surface reconstruction. These considerations are general and also apply to other systems. As/Sb covered Si(100) surfaces show subsurface strain patterns and core-level shifts qualitatively similar to the clean surface studied here [27]. From experimental work on strained Si layers deposited on Ge(100) and SiGe alloys, one derives that the Si $2p$ binding energy increases with tensile strain [28], in accord with the present analysis.

We now turn to the Si(100)-SiO_2 interface where the presence of highly electronegative O atoms might additionally affect the shifts of nonoxidized Si atoms [15]. As interface structure, we adopted model C′ from Ref. [10], which incorporates several experimentally identified features, including a displacement pattern in the substrate consistent with ion-scattering measurements. Calculated binding energies are given in Fig. 2 along the direction orthogonal to the interface plane. The binding energies of oxidized Si atoms increase almost linearly with the oxidation state [13,14], and show quantitative agreement with experimental values (Table III). The focus of the present investigation is on nonoxidized Si atoms, which give shifts with a significant spread near the interface. The simulated spectrum associated to these Si atoms could be decomposed into three components (Fig. 2, inset), yielding shifts for Si^{α} and Si^{β} in very good agreement with experimental data (Table III).

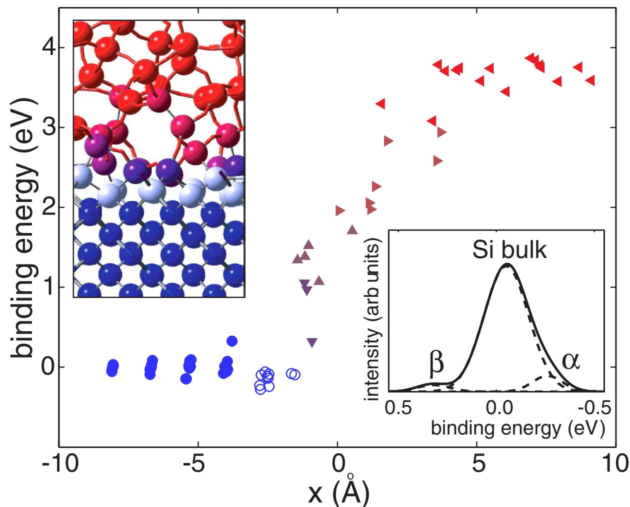

FIG. 2 (color online). Calculated Si $2p$ shifts at the Si(100)-SiO_2 interface along an orthogonal direction to the interface. The Si^{+n} correspond to oxidized Si atoms with n O neighbors ($n = 1$, ▼; 2, ▲; 3, ▶; 4, ◀) and are color-coded in the atomistic model. Nonoxidized Si atoms (Si^0) with (○) and without (●) second-neighbor O atoms are distinguished. Inset: simulated spectrum for Si^0 (Gaussian broadened: $\sigma = 0.08$ eV) and its decomposition in three components.

Following the same analysis as for the Si(100)-(2×1) surface, we identify second-neighbor electronegativity effects at the interface by monitoring deviations between the positions of bond centers and Wannier centers. For each nonoxidized Si atom, we correlate in Fig. 3(a) the distances to these two centers, distinguishing nonoxidized Si atoms with and without second-neighbor O atoms. In the absence of second-neighbor O atoms the Wannier center almost coincides with the Si-Si bond center, indicating that the electronegativity of O atoms does not affect third-neighbor bonds. However, for Si^* atoms with second-neighbor O atoms, the Wannier center systematically moves closer to the Si^* atom. This behavior is understood by considering that the central Si atom in a Si^*-Si-O unit requires a contribution from its $4s$ atomic orbital in order to accommodate the polarity in its Si-O bond, which in turn displaces the Wannier center of the Si^*-Si bond towards Si^*. In an equivalent way, this effect can be explained within the backdonation picture [29].

The displacement of the electron density towards the Si atom causes a decrease of its binding energy as can clearly be seen in Fig. 2, where all the Si atoms with second-neighbor O atoms show negative shifts. Hence, a highly electronegative atom in the *second*-neighbor shell causes an *opposite* effect on the shift as compared to such an atom in the *first*-neighbor shell [14]. Consequently, Si atoms with second-neighbor O atoms contribute to the Si^{α} line on the low binding energy side of the Si bulk line.

We now focus on nonoxidized Si atoms without second-neighbor O atoms. Figure 3(b) shows that for these atoms a linear relation holds between their core-level shift and their average Si-Si bond distance, in a similar way as for the Si(100)-(2×1) surface. We deduce that these shifts are the result of bond-length variations induced in the substrate by

TABLE III. Calculated and measured Si $2p$ shifts at the Si(100)-SiO_2 interface. The Si bulk line is taken as reference.

	Theory	Experiment	
	Present	Ref. [16]	Ref. [17]
α	−0.21	−0.25	−0.22
β	0.32	0.20	0.34
+1	0.78	1.00	0.95
+2	1.40	1.82	1.78
+3	2.37	2.62	2.60
+4	3.64	3.67	3.72

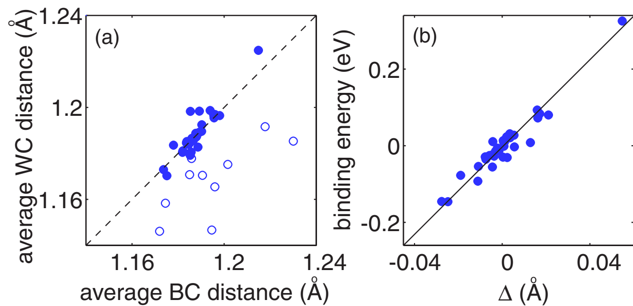

FIG. 3 (color online). Correlations for nonoxidized Si atoms at the Si(100)-SiO_2 interface: (a) average distance to the WC vs average distance to the Si-Si BC; (b) Si $2p$ shift vs average Si-Si bond length given as deviation (Δ) from the bulk value. Closed (open) symbols indicate Si atoms without (with) second-neighbor O atoms.

the disordered oxide. Contracted bonds give negative shifts and contribute to the Si^{α} component, in addition to second-neighbor electronegativity effects. On the contrary, bond elongations cause shifts towards higher binding energies, being at the origin of the Si^{β} component. From the experimental shift of about 0.3 eV, we infer the occurrence of Si atoms with an average bond-length elongation of ~0.05 Å.

Our analysis suggests that Si atoms contributing to the Si^{α} line should on average be closer to the oxide than those contributing to Si^{β}, at variance with a recent photodiffraction measurement favoring the opposite ordering [17]. However, the different sources of the Si^{α} line together with the nonabrupt nature of the interface might lead to intermixing of Si^{α} and Si^{β} atoms, resulting in depth profiles at the limit of experimental resolution.

In conclusion, we revealed the mechanisms underlying the fine structure in Si $2p$ photoelectron spectra at silicon surfaces and interfaces. A key result of our work is that photoelectron spectroscopy when combined with first-principles calculations can provide an atomic-scale probe of structural strain, resulting in a new functionality in addition to the detection of chemical composition.

The authors thank J. P. Chang, S. Dreiner, A. Stirling, and H. W. Yeom for fruitful interactions. The computational resources were provided by the DIT at EPFL.

[1] F. J. Himpsel *et al.*, in *Proceedings of the International School of Physics Enrico Fermi*, edited by M. Campagna and R. Rosei (Elsevier, Amsterdam, 1990), p. 203.
[2] E. Landemark, Y.-C. Chao, and R. I. G. Uhrberg, Phys. Rev. Lett. **69**, 1588 (1992).
[3] P. De Padova *et al.*, Phys. Rev. Lett. **81**, 2320 (1998).
[4] T.-W. Pi, C.-P. Cheng, and I.-H. Hong, Surf. Sci. **418**, 113 (1998).
[5] H. Koh *et al.*, Phys. Rev. B **67**, 073306 (2003).
[6] E. Pehlke and M. Scheffler, Phys. Rev. Lett. **71**, 2338 (1993).
[7] G. Jayaram, P. Xu, and L. D. Marks, Phys. Rev. Lett. **71**, 3489 (1993).
[8] J. E. Northrup, Phys. Rev. B **47**, 10 032 (1993).
[9] E. L. Bullock *et al.*, Phys. Rev. Lett. **74**, 2756 (1995).
[10] A. Bongiorno *et al.*, Phys. Rev. Lett. **90**, 186101 (2003).
[11] S. Dreiner, M. Schürmann, and C. Westphal, Phys. Rev. Lett. **93**, 126101 (2004).
[12] A. Bongiorno and A. Pasquarello, Phys. Rev. Lett. **94**, 189601 (2005); S. Dreiner, M. Schürmann, and C. Westphal , Phys. Rev. Lett. **94**, 189602 (2005).
[13] F. J. Himpsel *et al.*, Phys. Rev. B **38**, 6084 (1988).
[14] A. Pasquarello, M. S. Hybertsen, and R. Car, Phys. Rev. Lett. **74**, 1024 (1995); Phys. Rev. B **53**, 10 942 (1996).
[15] F. Jolly *et al.*, J. Non-Cryst. Solids **280**, 150 (2001).
[16] J. H. Oh *et al.*, Phys. Rev. B **63**, 205310 (2001).
[17] S. Dreiner, M. Schürmann, and C. Westphal, J. Electron Spectrosc. Relat. Phenom. **144–147**, 405 (2005).
[18] N. Marzari and D. Vanderbilt, Phys. Rev. B **56**, 12 847 (1997).
[19] R. Car and M. Parrinello, Phys. Rev. Lett. **55**, 2471 (1985); CPMD version 3.9.1, Copyright IBM Corp 1990-2004, Copyright MPI für Festkörperforschung Stuttgart 1997-2001, http://www.cpmd.org.
[20] N. Troullier and J. L. Martins, Phys. Rev. B **43**, 1993 (1991).
[21] D. Vanderbilt, Phys. Rev. B **41**, 7892 (1990); A. Pasquarello *et al.*, Phys. Rev. Lett. **69**, 1982 (1992); K. Laasonen *et al.*, Phys. Rev. B **47**, 10 142 (1993).
[22] D. R. Hamann and D. A. Muller, Phys. Rev. Lett. **89**, 126404 (2002).
[23] We performed all-electron calculations with the code ADF [24] using triple-zeta doubly polarized Slater orbitals.
[24] G. te Velde *et al.*, J. Comput. Chem. **22**, 931 (2001); C. F. Guerra *et al.*, Theor. Chem. Acc. **99**, 391 (1998); ADF2004.01, SCM, Theoretical Chemistry, Vrije Universiteit, Amsterdam, The Netherlands, http://www.scm.com.
[25] The loss of accuracy in previous calculations on the same molecules [14] resulted from the use of analytically interpolated pseudopotentials [G. B. Bachelet, D. R. Hamann, and M. Schlüter, Phys. Rev. B **26**, 4199 (1982)].
[26] Our reasoning applies to covalently bonded systems. An opposite dependence on strain is found for $3d$-metal clusters due to hybridization effects [B. Richter *et al.*, Phys. Rev. Lett. **93**, 026805 (2004)].
[27] J.-H. Cho, M.-H. Kang, and K. Terakura, Phys. Rev. B **55**, 15 464 (1997); J.-H. Cho and S. B. Zhang, Phys. Rev. Lett. **82**, 4564 (1999).
[28] E. T. Yu *et al.*, Appl. Phys. Lett. **56**, 569 (1990); L. D. Laude, F. H. Pollak, and M. Cardona, Phys. Rev. B **3**, 2623 (1971).
[29] J. A. Pople and M. Gordon, J. Am. Chem. Soc. **89**, 4253 (1967).
[30] The projections of $4'u$ ($4'd$) atoms on the surface plane lie between $1d$ ($1u$) atoms of different dimer rows.